Mechanics Research Communications 36 (2009) 75–81

Contents lists available at ScienceDirect

Mechanics Research Communications

journal homepage: www.elsevier.com/locate/mechrescom

Electro-osmotic flow control for living cell analysis in microfluidic PDMS chips

Tomasz Glawdel, Carolyn L. Ren *

Department of Mechanical and Mechatronics Engineering, University of Waterloo, 200 University Avenue W., Waterloo, Ontario, Canada N2L 3G1

ARTICLE INFO

Article history:
Received 7 April 2008
Received in revised form 20 June 2008
Available online 10 July 2008

Keywords:
Electro-osmotic pump
Microfluidic platform
Living cell analysis
Gel salt bridge

ABSTRACT

This study presents a microfluidic PDMS platform for multiplex cell culture applications. This platform includes two cell culture lines each of which consists of an integrated electro-osmotic pump, a cell culture chamber and a series of microchannels and reservoirs. Each integrated electro-osmotic pump consists of 70 parallel channels of 50 μm wide × 2.7 μm high, two electrode reservoirs and two gel salt bridges separating the electrode reservoirs and the parallel microchannels. In this design, efforts were made to address the problems associated with the use of high electric fields required for operating electro-osmotic pumps in living cell analysis. In particular, electroporation of cell membranes, Joule heating, electrolysis, bubbles and induced pressure disturbance were carefully considered through the design of the platform. The integrated electro-osmotic pumps allow the platform to be operated in three differential modes aiming to achieve flexible flow rate control and accurate injection of a small amount of reagent both of which are important for dynamic studies of cells.

1. Introduction

Microfluidic platforms enable living cell analysis with unprecedented control over environmental cues that influence cells largely due to a decrease in overall size (Park et al., 2007; Lu et al., 2004; El-Ali et al., 2006). Most of these microfluidic platforms employ pressure-driven flow as a pumping method. A typical example of a pressure-driven microfluidic platform consisting of a channel network and an external pump either syringe (Kim et al., 2006), peristaltic (Leclerc et al., 2004) or gravity (Zhu et al., 2004) connected *via* tubing, connectors and valves as shown in Fig. 1. In this design, the overall flow rate to the platform can be controlled; however, the flow rate to each cell chamber is governed by the relative hydrodynamic resistance of the channels. The use of off-chip valves and pumps suffers from long response times due to the dead volume of the components and the elasticity of the tubing and microchannels especially if they are made of soft polymers. Consequently, this setup lacks the fine temporal and spatial flow control that is required for dynamic studies of cells involving multiple media sources and discrete injections of small amounts of fluids such as drugs.

A few examples exist for highly functional pressure-driven flow control systems. Futai et al. (2006) developed a recirculating perfusion platform using a Braille display to pump and small pins to deflect PDMS channels for valving. Braschler et al. (2007) showed precise control over a hydrodynamic focuser using pressure bombs which increase the atmospheric pressure in a sealed fluid reservoir. The most successful pumping system is that developed by Quake's group, which uses micromechanical elastomeric valves that are pneumatically controlled in a bi-layer PDMS chip. For example, Gomez-Sjoberg et al.

* Corresponding author. Tel.: +1 519 888 4567x33030; fax: +1 519 885 5862.
E-mail address: c3ren@mecheng1.uwaterloo.ca (C.L. Ren).

0093-6413/$ - see front matter © 2008 Elsevier Ltd. All rights reserved.
doi:10.1016/j.mechrescom.2008.06.015

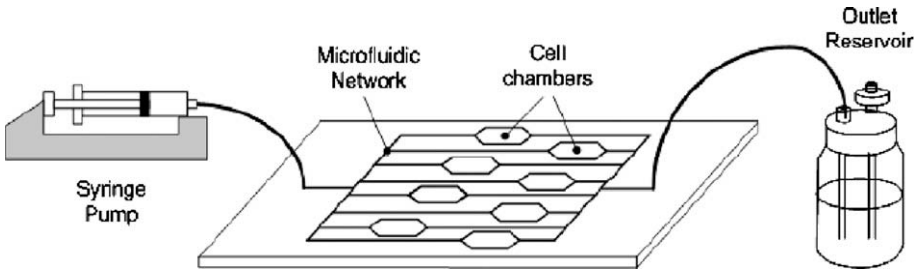

Fig. 1. Schematic of typical pressure-driven microfluidic platform for living cell analysis using an external syringe pump to supply medium.

(2007) presented a fully automated multiplexed cell culture system with 96 culture chambers and 16 reagent streams that can be mixed using such on-chip valves and pumps.

Besides pressure-driven flow, electro-osmotic flow (EOF) is another common pumping method for microfluidic platforms. EOF occurs when an electric field is applied tangentially to the electric double layer (EDL) which forms when a liquid comes in contact with a solid surface. Ions in the EDL migrate towards the appropriate electrode and generate fluid flow through viscous drag. The velocity profile is uniform in the bulk except within the EDL. Typically, the EDL is several orders of magnitude smaller than the channel dimensions so that the fluid appears to slip by the surface. Under such conditions the Helmholtz–Smoluchowski equation gives the slip velocity, $u = \mu_e E_x$, where E_x is the applied electric field strength and μ_e is the electro-osmotic mobility which is a unique property of the solid–liquid paring.

EOF is a compact method where flow rate and direction can be accurately controlled in a large microchannel network by simply manipulating the applied voltages at the reservoirs connected to the microchannels. The temporal response of EOF is on the order of milliseconds and femto-liter resolution can also be achieved (Yan et al., 2006). Unlike integrated membrane-based valves and peristaltic pumps there are no moving parts or pulsating flow in EOF. The above-mentioned features allow for the possibility of performing dynamic studies with cells by precisely manipulating the flow rate and medium to each cell chamber. However, EOF has not been applied to living cell analysis for a variety of reasons. Mostly notably the high electric fields associated with EOF cause electroporation of cell membranes (Lee and Cho, 2007), the high ionic concentration typical to cell culture medium may result in excessive Joule heating (Xuan et al., 2004), and bubbles and electrolysis (Rodriguez and Chandrasekhar, 2005) due to large current draws. These effects will result in dynamic changes in the liquid temperature and pH value causing instability of EOF performance. Therefore, to utilize the advantages of EOF for living cell analysis, these problems should be addressed by integrating electro-osmotic (EO) pumps on-chip which generates pressure-driven flow from EOF.

This work focuses on discussing the challenges in applying EO pumps to living cell analysis while demonstrating their potential. For this purpose a microfluidic platform based on controlling fluid flow with integrated electro-osmotic (EO) pumps is presented for culturing cells on chip. This platform consists of two cell culture lines each of which contains an EO pump connected to a cell chamber and then merge together by a manifold. The design and operation of the microfluidic chip with integrated EO pumps was modeled using compact circuit modeling of EOF and pressure-driven flow (Qiao and Aluru, 2002). These models are compared to full numerical models to demonstrate their accuracy in modeling flow in microchannel networks and are then applied to describe the operation of the EO pumps in a living cell analysis chip.

2. Principles of electro-osmotic pump

As mentioned above high electrical fields must be avoided in the cell culture area to avoid electroporation of cell membranes, which can be achieved by using EO pumps to generate pressure-driven flow in the area with cells. The flow rate passing through the cells can be manipulated by altering the flow rate of the EO pumps. A few EO pumps have been developed to induce pressure-driven flow, most of which are stand alone devices used for drug dispensing. These devices are based on porous structures, employing either glass frits (Yao et al., 2003; Yao and Santiago, 2003), columns packed with silica beads (Chen et al., 2004), monoliths (Tripp et al., 2004) or silicon membranes (Yao et al., 2006) to generate EOF. Since integrating porous structures into a planar microfluidic platform is difficult, they are replaced by a number of parallel microchannels in the proposed design similar to that presented by Chen and Santiago (2002).

Fig. 2 shows a simplified schematic of a planar EO pump which can be decomposed into five main regions: Ch1 and Ch3 are the inlet and outlet channels, respectively, and Ch2 is the EOF region connected to the electrode reservoirs at its two ends (Ch4 and Ch5). In this design, the applied electric field generates EOF in the Ch2 region which generates an internal pressure difference drawing fluid *via* a vacuum into the pump and pushing fluid *via* positive pressure out of the pump. The fluid flow in the EOF region is actually a combination of EOF and backflow caused by the pressure difference. Membranes are often employed in such an EO pump to separate the electrode reservoirs and the EOF region to prevent electrolysis byproducts (H^+, OH^- and bubbles) entering the fluid region.

Simplified compact circuit models are typically used for analysis and design of global microfluidic networks as these require little computational effort while are still accurate enough to capture the basic phenomena. Compact circuit models has

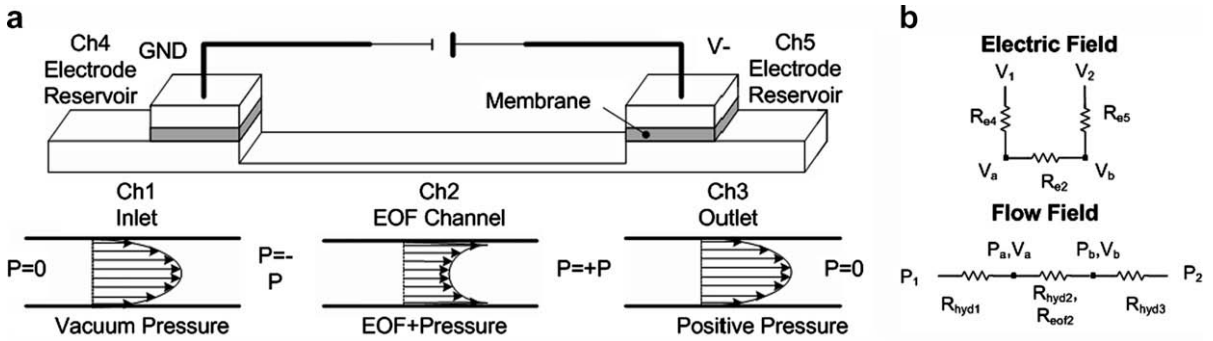

Fig. 2. (a) Schematic representing the operating principals of planar EO pumps. (b) Equivalent electrical and flow circuit models of the EO pumps.

been applied to solve the flow field in microfluidic networks using EOF (Qiao and Aluru, 2002) and combined pressure driven/EOF (Xuan and Li, 2004). The conditions of using this model include that the flow is laminar and the Navier-Stokes equations become linear, which are true for most planar EO pumps for the majority of liquids. When applying these models to a planar EO pump, the pump network can be decomposed into two equivalent circuits that describe the electric field and the flow field (see Fig. 2b). The two circuits are solved using the nodal analysis technique typically employed in electrical engineering. The flow rate and pressure difference generated by the EO pump are given as:

$$Q = (IR_{e_2}/R_{\mathrm{eof}_2})[R_{\mathrm{hyd}_2}/(R_{\mathrm{hyd}_1} + R_{\mathrm{hyd}_2} + R_{\mathrm{hyd}_3})] \quad (1)$$

$$P_{\mathrm{b}} - P_{\mathrm{a}} = Q(R_{\mathrm{hyd}_1} + R_{\mathrm{hyd}_2}) \quad (2)$$

where I is the applied current, R_e is the electrical resistance, $R_e = L/(\sigma wh)$, R_{eof} the electro-osmotic resistance, $R_{\mathrm{eof}} = L/(\mu_e \mathrm{wh})$, and R_{hyd} the pressure resistance of the channel, $R_{\mathrm{hyd}} = 12\ \mu\mathrm{L}/(wh^3)$. The parameters involved here include the electrical conductivity σ, the viscosity μ, the electro-osmotic mobility μ_e, the channel length L, width w and height h. The analysis above assumes a thin EDL and that the Helmholtz–Smoluchowski equation is valid in the EOF region. To achieve a high flow rate using low voltages the EOF carrying channel must have a high pressure resistance and a low electro-osmotic resistance compared to the inlet and outlet channels. This is accomplished by designing EOF carrying channels that are short, wide and very shallow. In addition, the channels should be large so that they have a low electrical resistance reducing the electrical field loss in these channels.

3. EO pump designed for cell culture solutions

A new generation pump was designed using the compact circuit model with specific criteria considered for continuous medium perfusion for cell culture (Glawdel, 2007). The perfusion medium contains the following concentration of components: 136 mM NaCl, 5 mM KCl, 1.6 mM $MgSO_4$, 2.1 mM $MgCl_2$, 1.26 mM $CaCl_2$, 1.3 mM Na_2HPO_4, 0.36 mM KH_2PO_4, 5 mM Galactose and 6.7 mM Pyruvate. The electrical conductivity was measured was relatively high 1.10 S/m and the electro-osmotic mobility measured using the current monitoring technique (Sze et al., 2003) was low 1.34×10^{-8} $\mathrm{m}^2/(\mathrm{Vs})$. The EO pump developed for pumping the medium is shown in Fig. 3. The EOF region consists of 70 parallel channels of 50 μm wide × 2.7 μm high while the other areas are 80 μm in height. The size and number of EOF channels was determined to generate a modest flow rate of 1 μL/min for an applied current of 300 μA or 300 V. A number of posts were added to the gel salt bridge region to increase the mechanical stability of the gel bridge. The overall size of the pump is approximately 1 cm × 2.5 cm. On one microscope slide four of these pumps can be comfortably fabricated for multiplex operation.

The largest issue plaguing EO pumps is the lack of long-term stability during continuous operation caused by electrolysis at the electrodes (Brask et al., 2005). Electrolysis generates excessive H^+ and OH^- ions dynamically changing the local pH value which will change the electro-osmotic mobility causing perturbations in EOF (Kirby and Hasselbrink, 2004). The ion generation also increases the conductivity of the working liquid (Rodriguez and Chandrasekhar, 2005) which in turn speeds up electrolysis. Moreover, the electrolysis reaction consumes water and generates bubbles in the reservoirs which will stop EOF after a long period of operation because the electrode will lose contact with the fluid either due to bubbles or due to water depletion. The electrolysis effects on the EO pump performance are minimized in this design through the following two approaches. First, incorporating gel salt bridges (serving as membranes) to separate the electrode reservoirs from the EOF carrying channels which will prevent or delay electrolysis byproducts entering the EOF channels. In this design, gel salt bridges are used to replace commercial ion exchange membranes which are typically used in EO pumps (Liu et al., 2003; Brask et al., 2005) because integrating commercial membranes is difficult in polydimethylsiloxane (PDMS) platforms due to inherent swelling and sealing issues (Jonsson and Lindberg, 2006). The gel salt bridges were fabricated using the method reported by Takamura et al. (2003). Second, mounting large reservoirs (2 ml) onto the electrode reservoirs and filling them with a well buffered solution of Bufferall (Sigma-Aldrich) to absorb electrolysis effects which will prolong the EO pump

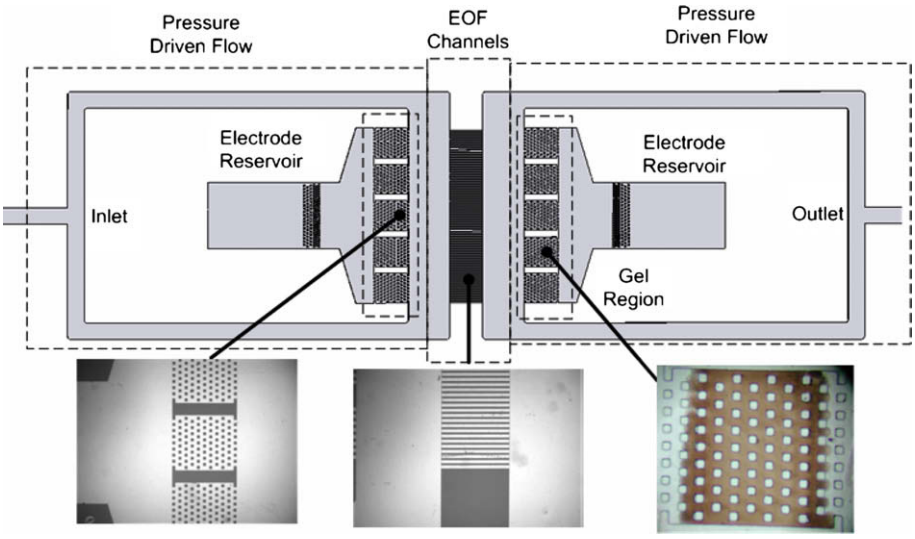

Fig. 3. Diagram of the EO pump design and images of each component fabricated in PDMS.

Table 1
Comparison of experimental, 3D numerical and compact circuit model results for 1XTBE

Current (μA)	Flow rate (μL/min)		
	Exp	Numerical model	Compact model
68	1.098 ± 0.055	1.088	1.096
140	2.08 ± 0.11	2.24	2.257

operation (de Jesus et al., 2005). An estimate of the depletion time of the buffer is given as $\tau_{dep} = cv_{res\ F}/I$ (Brask et al., 2005), where F is the Faradays constant, v_{res} is the reservoir volume, I is the electric current (500 μA) and c the buffer concentration (100 mM). With these values the depletion time in this study is approximately 10.7 h which is still much lower than conventional cell culture perfusion requirements of 1–7 days. Once the buffer is depleted significant changes in pH will occur at the reservoirs resulting in changes to the zeta potential and flow. Therefore, the buffer should be replaced prior to this time limiting this design.

To improve the EO pump stability, a few other features are incorporated into this design. First, the EOF carrying channels are designed to be wide and shallow (50 μm wide × 2.7 μm high) to suppress induced pressure disturbances from the differences in hydraulic head and menisci in the electrode reservoirs and to minimize Joule heating effects due to its large surface-to-volume ratio. Second, the EO pumps are operated in a constant current mode to ensure that the same electric field will always be applied across the EOF channels when bubbles form (Brask et al., 2005).

To justify the use of compact circuit analysis model for an EO pump design, a 3D numerical model was also developed and solved using the COMSOL Multiphysics module for comparison. The flow rate in the inlet region of the channel network was predicted using this 3D model and compared with experimental results and the compact circuit model results. In the experiments, the flow rate was obtained by visualizing the motion of the 0.2 μm fluorescent beads (Fluoresbrite YG, Molecular Probes) added to the working fluid using a fluorescent visualization system. Five successive images were taken at the middle channel height at the inlet of the pump where only pressure-driven flow exists since the electric field in the EOF region would also impose an electrophoretic velocity on the beads. The flow rate was estimated using the centerline flow velocity through the equation for Poiseuille flow between parallel plates. Table 1 summarizes the comparison of the models and experimental results for several applied currents using the buffer solution 1×TBE (tris-borate-EDTA). The predicted flow rates from the two models are in excellent agreement, which indicates that the compact circuit model is sufficient for design purposes. Comparing the model predicted results with experimental values there is also a good agreement. Small discrepancies might be due to uncertainties in measuring flow rate.

4. Integration of EO pumps into cell culture network

Fig. 4 shows the image of the fabricated microfluidic platform proposed using the compact circuit model. The channel network incorporates two cell culture lines each of which consists of one cell chamber, one EO pump and four reservoirs. A shallow intersecting channel is designed to connect the two cell lines and the inlet channel (R1) and to prevent cross flow

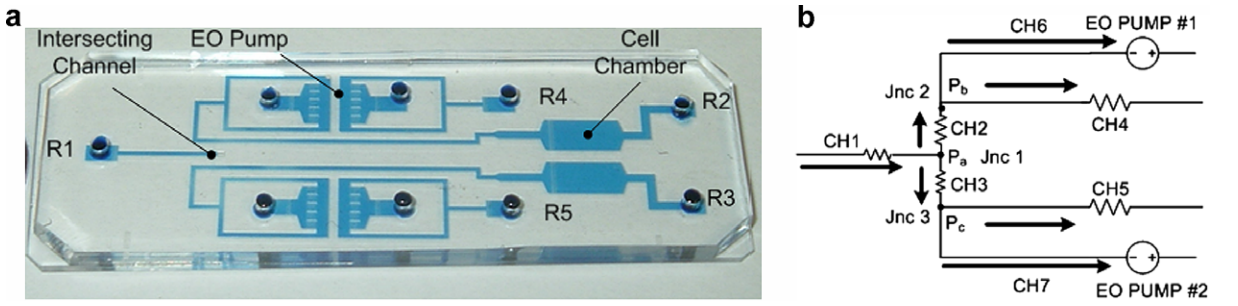

Fig. 4. (a) Fabricated microfluidic network in PDMS with dye added to visualize the network and (b) circuit model of the fluid network.

between the two cell lines. The cell chambers were designed to have the same surface area as a conventional 96 well plate and their tapered inlets/outlets provide a more uniform velocity field across the cell area (rectangular portion). Since the microfluidic platform involves three different channel heights: 2.7 μm for EOF channels, 5.1 μm for the intersecting channel and 80.2 μm for the other channels, it was fabricated from a multi-level SU-8 master using standard soft lithography techniques.

To describe the operation of the microfluidic network the compact circuit analysis can also be applied. Referring to Fig. 4b, the system of equations that describe the flow network is:

$$Q_1 = (P_1 - P_a)/R_{hyd_1} \quad \text{(inlet channel)}, \quad Q_5 = P_c/R_{hyd_5} \quad \text{(cell chamber channel)}$$
$$Q_2 = (P_a - P_b)/R_{hyd_2} \quad \text{(branch channel)}, \quad Q_6 = P_b/R_{hyd_6} + G_{EOP_1} I_{EOP_1}/R_{hyd_6} \quad \text{(EO Pump\#1channel)}$$
$$Q_3 = (P_a - P_c)/R_{hyd_3} \quad \text{(branch channel)}, \quad Q_7 = P_c/R_{hyd_7} + G_{EOP_1} I_{EOP_2}/R_{hyd_7} \quad \text{(EO Pump\#2channel)}$$
$$Q_4 = P_b/R_{hyd_4} \quad \text{(cell chamber channel)}, \quad Q_1 = Q_2 + Q_3, \quad Q_2 = Q_4 + Q_6, \quad Q_3 = Q_5 + Q_7$$

I_{EOP} is the constant current applied to operate the pump and G_{EOP} is a geometric factor of the EO pump derived from the network analysis for the pump and is given as:

$$G_{EOP} = R_{hyd_2} R_{e_2}/R_{eof_2} \tag{3}$$

where the resistances refer to the EOF channels in the EO pump. The benefit of integrating EO pumps in the platform is the added versatility that they offer in controlling fluid flow. For this chip there exist three potential modes for using EO pumps to control the flow to the cell chambers, as shown in Fig. 5.

4.1. Mode #1

In this mode (see Fig. 5a), the two EO pumps are operating independently without an external flow source. They draw liquid from R2 and R3 into the cell chambers and then through the EO pumps. This is the preferred method of pumping as opposed to the opposite where the fluid is pumped from R4 and R5 where the medium may change in temperature or composition by passing through the EO pumps. The electrode near the cell chamber is set to ground (GND) and the other to a negative voltage (−V) to prevent the cells experiencing an abnormally high voltage. The cells experience a slightly

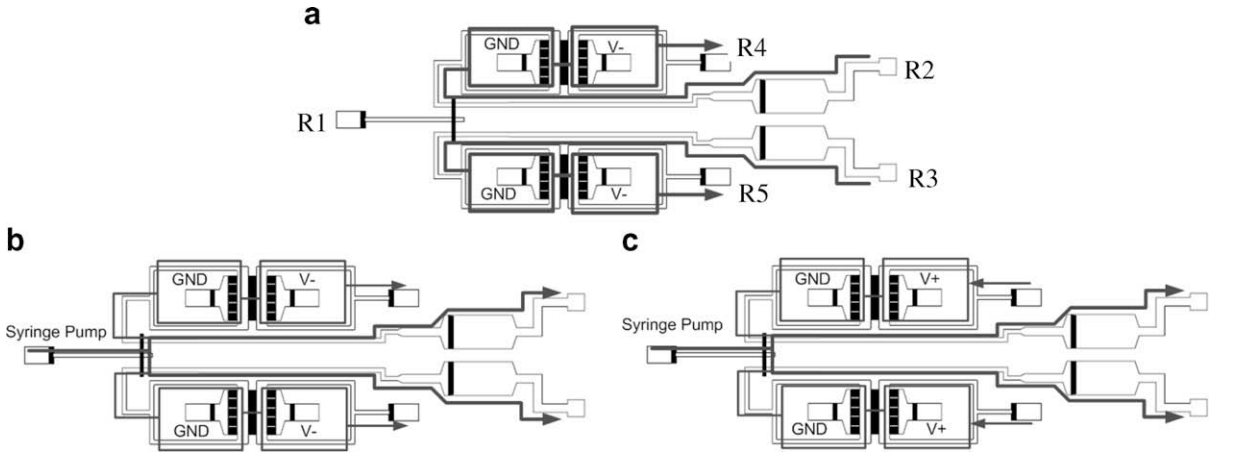

Fig. 5. Three operational modes of the microfluidic network (a) EO pump operates independently, (b) EO pumps regulate flow from another principal source to the cell culture chambers, and (c) EO pumps inject fluid continuously or discretely into the main fluid flow.

negative pressure (a few Pascals) since they are at the inlet side of the EO pump. Since the intersecting channels (CH2, CH3) are of high resistance compared to the cell culture channels (CH4, CH5) the two pumps are essentially isolated from each other. Solving the system of equations where $Q_1 = 0$, $Q_2 = 0$, $Q_3 = 0$, the flow rate to the two chambers are:

$$Q_4 = -I_{EOF\#1} G_{EOF\#1} / (R_{hyd_6} + R_{hyd_4}) \tag{4}$$

$$Q_7 = -I_{EOF\#2} G_{EOF\#3} / (R_{hyd_5} + R_{hyd_7}) \tag{5}$$

The negative sign indicates that the fluid flow will be opposite to the direction in Fig. 5a.

4.2. Mode #2

In this mode shown in Fig. 5b, a syringe pump provides the main liquid flow to the channel network at a constant flow rate, Q_1. Due to symmetry between the two cell lines the flow will split equally entering into the two cell lines ($Q_2 = Q_3 = Q_1/2$). Little flow will be lost to the EO pumps channels due to their high hydrodynamic resistance compared to the cell chambers. This setup is the same as that used in previous cell culture devices where the flow rate to the chamber is fixed. However, with the EO pumps the flow rate to the cell chamber can be manipulated by altering the EO pumping flow rate. Using the compact circuit model, the flow rates of the rest of the channel network can be determined assuming the desired flow rate for each cell line is known. Firstly, the internal pressures P_b and P_c can be calculated using the equations for junctions 2 and 3 ($Q_1 = Q_2 + Q_3$, $Q_2 = Q_4 + Q_6$):

$$P_b = \left(\frac{P_a}{R_{hyd_2}} - \frac{G_{EOP_1}}{R_{hyd_6}} I_{EOP_1} \right) \left(\frac{R_{hyd_2} R_{hyd_4} R_{hyd_6}}{R_{hyd_2} R_{hyd_4} + R_{hyd_2} R_{hyd_6} + R_{hyd_4} R_{hyd_6}} \right) \tag{6}$$

$$P_c = \left(\frac{P_a}{R_{hyd_3}} - \frac{G_{EOP_2}}{R_{hyd_7}} I_{EF_2} \right) \left(\frac{R_{hyd_3} R_{hyd_5} R_{hyd_7}}{R_{hyd_3} R_{hyd_5} + R_{hyd_3} R_{hyd_7} + R_{hyd_5} R_{hyd_7}} \right) \tag{7}$$

Applying the equation at junction 1 to solve for P_a:

$$Q_1 = (P_a - P_b)/R_{hyd_2} + (P_a - P_c)/R_{hyd_3} \tag{8}$$

Substituting P_a and P_b into the equation leads to

$$P_a = \frac{R_{hyd_2}}{2(1 - K_f)} \left[Q_1 - \frac{G_{EOP}}{R_{hyd_6}} K_f (I_{EOP\#1} + I_{EOP\#2}) \right] \tag{9}$$

where $K_f = R_{hyd_4} R_{hyd_6} / (R_{hyd_2} R_{hyd_4} + R_{hyd_2} R_{hyd_6} + R_{hyd_4} R_{hyd_6})$. Recalling that the hydrodynamic resistance of the cell culture channel is much smaller than the intersection channel and the EO pump channels ($R_{hyd_4} \ll R_{hyd_2}, R_{hyd_6}$), K_f can be approximated as zero reducing Eq. (9) to $P_a \cong R_{hyd_2} Q_1/2$. This more importantly means that even with the EO pumps operating the flow rate from the syringe pump will split equally to the two cell lines: $Q_2 \cong Q_3 \cong Q_1/2$. This is due to the high resistance of the intersecting channel which isolates the two EO pumps from each other. The electrical currents required to achieve the desired flow rates to the cell chambers are:

$$I_{EOP\#1} = (Q_1/2 - Q_4)(R_{hyd_6}/G_{EOP\#1}) \tag{10}$$

$$I_{EOP\#2} = (Q_1/2 - Q_5)(R_{hyd_7}/G_{EOP\#2}) \tag{11}$$

Eqs. (10) and (11) imply an important condition for specifying the flow rates to the cell chambers, which is $0 < Q_4 < Q_1/2$, or the EO pumps will not draw fluid from the main stream but adding to it.

4.3. Mode #3

In the third configuration (see Fig. 5c), the EO pumps are used to dispense small amounts of fluids into the main stream either periodically or continuously. Therefore, the derivation is the same as that for mode #2 except the specified flow rate to the cell chamber must meet the condition: $Q_4 > Q_1/2$. The critical condition for stopping flow to the cell chamber is:

$$I_{EOP\#1} = (R_{hyd_6}/G_{EOP\#1})(Q_1/2) \tag{12}$$

As discussed above, using the compact circuit analysis the different operational modes of the EO pumps in the network can be defined. The EO pumps can act as either primary sources of fluid flow for injecting fluid into the main stream or drawing fluid over the cells as virtual valves that regulate the amount of flow to the cell chambers. Therefore, integrated EO pumps in a microfluidic platform can be used to provide dynamic control of the fluid within the network while suppressing many of the negative effects of EOF from the cells.

5. Concluding remarks

This study introduces the concept of merging the advantages of electro-osmotic flow (EOF) in a living cell analysis chip through the application of electro-osmotic pumps. Electro-osmotic pumps isolate the high electric field away from the cells

preventing electroporation and damage to the cells. The problems associated with the use of EO pumps for pumping cell culture medium such as electroporation, electrolysis, Joule heating and bubbles were discussed and a planar EO pump design was introduced for cell culture. To demonstrate the flexibility of using EO pumps, a microfluidic network for cell culture was presented and three different operation modes meeting the needs of dynamic studies of living cells were modeled using compact flow circuit techniques.

Acknowledgements

The authors greatly acknowledge the support of Natural Science and Engineering Research Council for a Grant to Carolyn L. Ren and a Postgraduate Scholarship to Tomasz Glawdel.

References

Braschler, T., Metref, L., Zvitov-Marabi, R., van Lintel, H., Demierre, N., Theytaz, J., Renaud, P., 2007. A simple pneumatic setup for driving microfluidics. Lab Chip 7, 420–422.
Brask, A., Kutter, J.P., Bruus, H., 2005. Long-term stable electroosmotic pump with ion exchange membranes. Lab Chip 5, 730–738.
Chen, C.H., Santiago, J.G., 2002. A planar electroosmotic micropump. J. Microelectromech. Syst. 11, 672–683.
Chen, L.X., Ma, J.P., Guan, Y.F., 2004. Study of an electroosmotic pump for liquid delivery and its application in capillary column liquid chromatography. Sensor Actuator, A 1028, 219–226.
de Jesus, D.P., Brito-Neto, J.G.A., Richter, E.M., Angnes, L., Gutz, I.G.R., do Lago, C.L., 2005. Extending the lifetime of the running electrolyte in capillary electrophoresis by using additional compartments for external electrolysis. Anal. Chem. 77, 607–614.
El-Ali, J., Sorger, P.K., Jensen, K.F., 2006. Cells on chips. Nature 442, 403–411.
Futai, N., Gu, W., Song, J.W., Takayama, S., 2006. Handheld recirculation system and customized media for microfluidic cell culture. Lab Chip 6, 149–154.
Glawdel, T., 2007. Design, Fabrication and Characterization of Electrokinetically Pumped Microfluidic Chips for Cell Culture Applications. Mechanical and Mechatronics Engineering. Waterloo, University of Waterloo. M.A.Sc: 222.
Gomez-Sjoberg, R., Leyrat, A.A., Pirone, D.M., Chen, C.S., Quake, S.R., 2007. Versatile, fully automated, microfluidic cell culture system. Anal. Chem. 79, 8557–8563.
Jonsson, M., Lindberg, U., 2006. A planar polymer microfluidic electrocapture device for bead immobilization. J. Micromech. Microeng. 16, 2116–2120.
Kim, L., Vahey, M.D., Lee, H.Y., Voldman, J., 2006. Microfluidic arrays for logarithmically perfused embryonic stem cell culture. Lab Chip 6, 394–406.
Kirby, B.J., Hasselbrink, E.F., 2004. Zeta potential of microfluidic substrates: 1. Theory, experimental techniques, and effects on separations. Electrophoresis 25, 187–202.
Leclerc, E., Sakai, Y., Fujii, T., 2004. Microfluidic PDMS (polydimethylsiloxane) bioreactor for large-scale culture of hepatocytes. Biotechnol. Prog. 20, 750–755.
Lee, D.W., Cho, Y.H., 2007. A continuous electrical cell lysis device using a low dc voltage for a cell transport and rupture. Sensor Actuator, B 124, 84–89.
Liu, S.R., Pu, Q.S., Lu, J.J., 2003. Electric field-decoupled electroosmotic pump for microfluidic devices. J. Chromatogr. A 1013, 57–64.
Lu, H., Koo, L.Y., Wang, W.C.M., Lauffenburger, D.A., Griffith, L.G., Jensen, K.F., 2004. Microfluidic shear devices for quantitative analysis of cell adhesion. Anal. Chem. 76, 5257–5264.
Park, J.Y., Hwang, C.M., Lee, S.H., Lee, S.H., 2007. Gradient generation by an osmotic pump and the behavior of human mesenchymal stem cells under the fetal bovine serum concentration gradient. Lab Chip 7, 1673–1680.
Qiao, R., Aluru, N.R., 2002. A compact model for electroosmotic flows in microfluidic devices. J. Micromech. Microeng. 12, 625–635.
Rodriguez, I., Chandrasekhar, N., 2005. Experimental study and numerical estimation of current changes in electroosmotically pumped microfluidic devices. Electrophoresis 26, 1114–1121.
Sze, A., Erickson, D., Ren, L.Q., Li, D.Q., 2003. Zeta-potential measurement using the Smoluchowski equation and the slope of the current–time relationship in electroosmotic flow. J. Colloid Interf. Sci. 261, 402–410.
Takamura, Y., Onoda, H., Inokuchi, H., Adachi, S., Oki, A., Horiike, Y., 2003. Low-voltage electroosmosis pump for stand-alone microfluidics devices. Electrophoresis 24, 185–192.
Tripp, J.A., Svec, F., Frechet, J.M.J., Zeng, S.L., Mikkelsen, J.C., Santiago, J.G., 2004. High-pressure electroosmotic pumps based on porous polymer monoliths. Sensor Actuator, B 99, 66–73.
Xuan, X.C., Li, D.Q., 2004. Analysis of electrokinetic flow in microfluidic networks. J. Micromech. Microeng. 14, 290–298.
Xuan, X.C., Xu, B., Sinton, D., Li, D.Q., 2004. Electroosmotic flow with Joule heating effects. Lab Chip 4, 230–236.
Yan, D.G., Nguyen, N.T., Yang, C., Huang, X.Y., 2006. Visualizing the transient electroosmotic flow and measuring the zeta potential of microchannels with a micro-PIV technique. J. Chem. Phys. 124.
Yao, S.H., Hertzog, D.E., Zeng, S.L., Mikkelsen, J.C., Santiago, J.G., 2003. Porous glass electroosmotic pumps: design and experiments. J. Colliod Interf. Sci. 268, 143–153.
Yao, S.H., Myers, A.M., Posner, J.D., Rose, K.A., Santiago, J.G., 2006. Electroosmotic pumps fabricated from porous silicon membranes. J. Microelectromech. Syst. 15, 717–728.
Yao, S.H., Santiago, J.G., 2003. Porous glass electroosmotic pumps: theory. J. Colliod Interf. Sci. 268, 133–142.
Zhu, X.Y., Chu, L.Y., Chueh, B.H., Shen, M.W., Hazarika, B., Phadke, N., Takayama, S., 2004. Arrays of horizontally-oriented mini-reservoirs generate steady microfluidic flows for continuous perfusion cell culture and gradient generation. Analyst 129, 1026–1031.